

Supporting information:

Superparticles of gold nanorods with controllable bandwidth and spectral shape for lipophilic SERS

Xun Li[†], Xi Chen[†], Jie Liu[†], Xiaoyu Zhao[‡], Jia Liu[‡], Zhiqun Cheng[†], Tian-Song Deng^{†,}*

**Corresponding author. E-mail: dengts@pku.edu.cn*

[†]School of Electronics and Information Engineering, Hangzhou Dianzi University, Hangzhou 310018, P. R. China.

[‡]College of Materials and Environmental Engineering, Hangzhou Dianzi University, Hangzhou 310018, P. R. China.

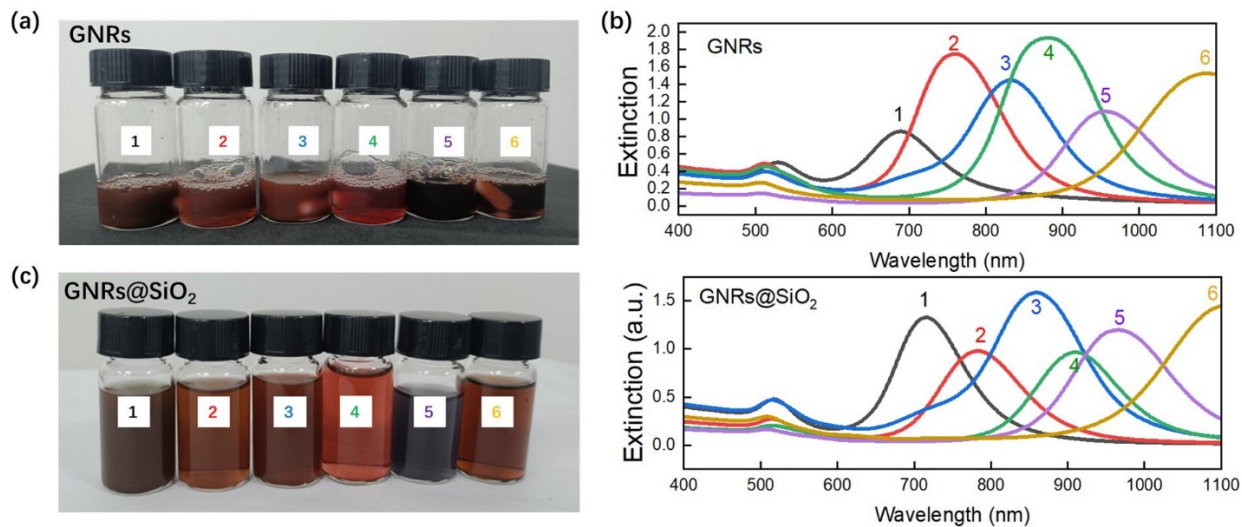


Fig. S1 Photographs and spectra of different GNRs and GNRs@SiO₂. (a) The prepared GNRs with six different LSPRs were dispersed in 1.5 mM CTAB, corresponding to Fig. 2a (1-6) of GNRs. (b) Measured spectra of the samples corresponding to GNRs in (a). (c) Six GNRs of different LSPRs were dispersed in ethanol solution after coating a mesoporous silica shell, corresponding to Fig. 2a (1-6) of GNRs@SiO₂. (d) Measured spectra of the samples corresponding to GNRs@SiO₂ in (c).

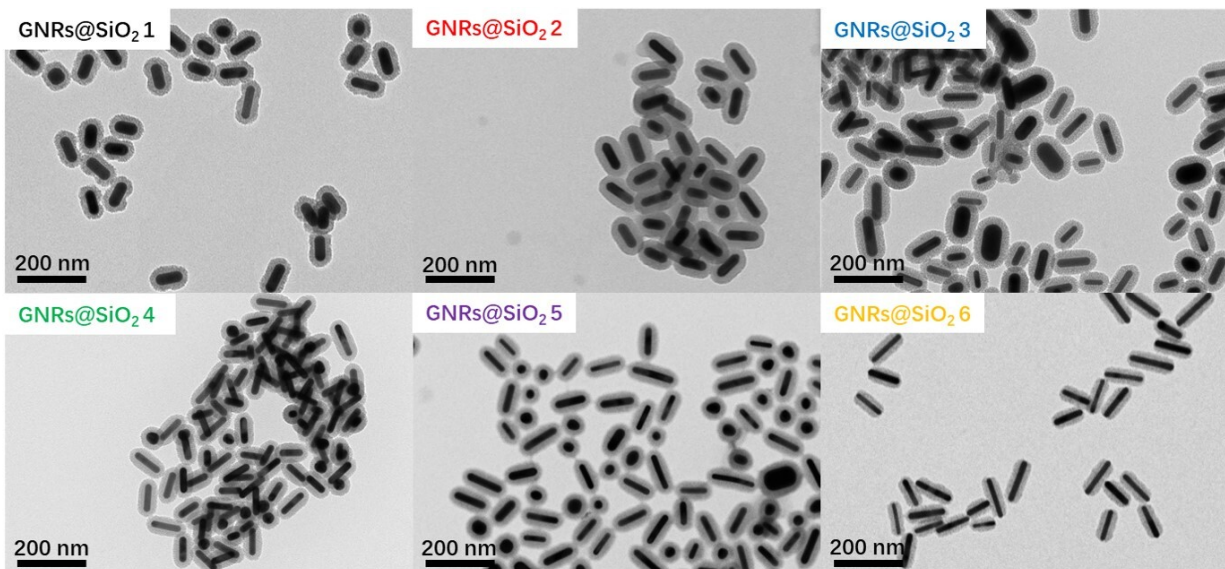


Fig. S2 TEM images corresponding to GNRs@SiO₂ 1-6 with different LSPRs in Fig. 2a.

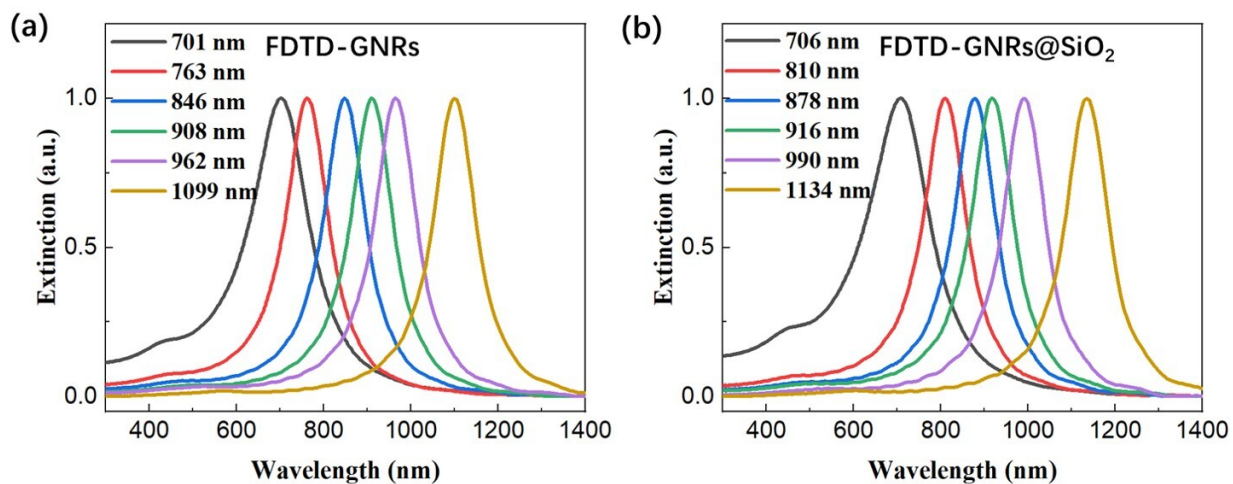


Fig. S3 FDTD simulated spectra. (a) FDTD simulated extinction spectra obtained by excitation of six GNRs of different LSPRs along the longitudinal axis. (b) FDTD simulated extinction spectra obtained by excitation of six GNRs@SiO₂ of different LSPRs along the longitudinal axis.

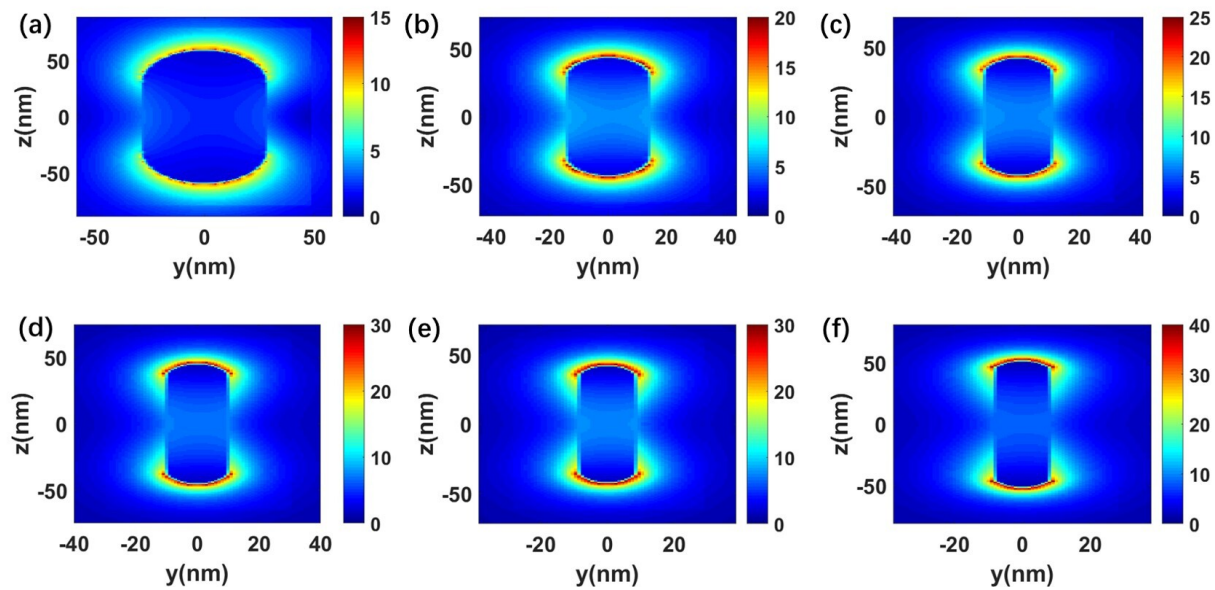


Fig. S4 FDTD simulations of the electric field distribution of single GNRs with different LSPRs, corresponding to Fig. 2a (1-6) of GNRs.

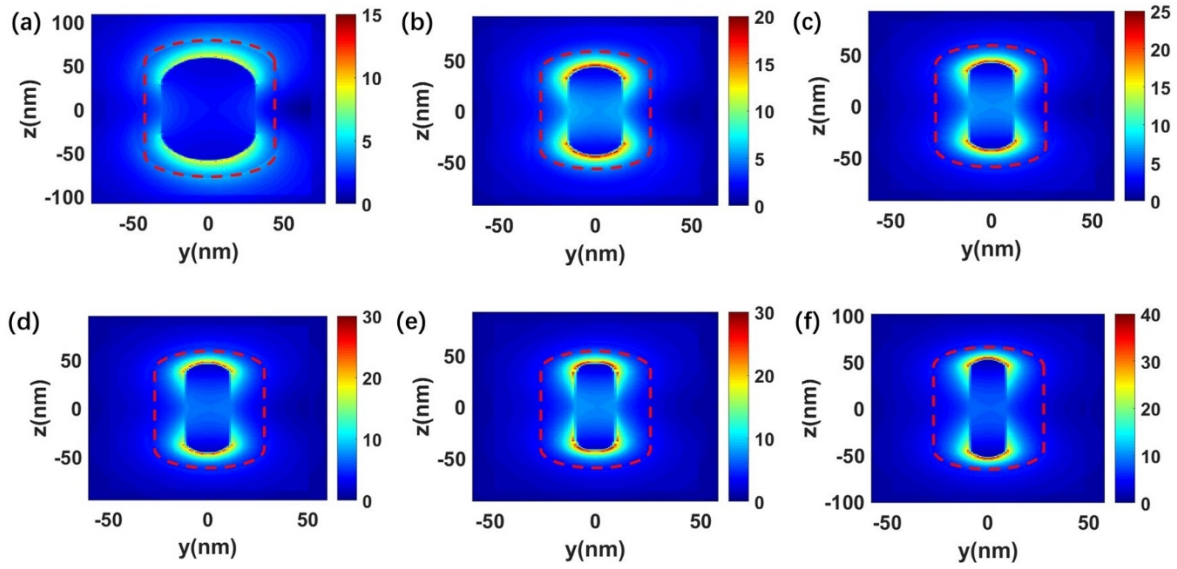


Fig. S5 FDTD simulations of the electric field distribution of a single GNRs@SiO₂ with different LSPRs, corresponding to Fig. 2a (1-6) of GNRs@SiO₂. There is a layer of mesoporous silica with a thickness of 20 nm on the surface of the GNRs, as shown in the figure between the red dotted line and the GNRs. The electric field outside the red dotted line is very weak.

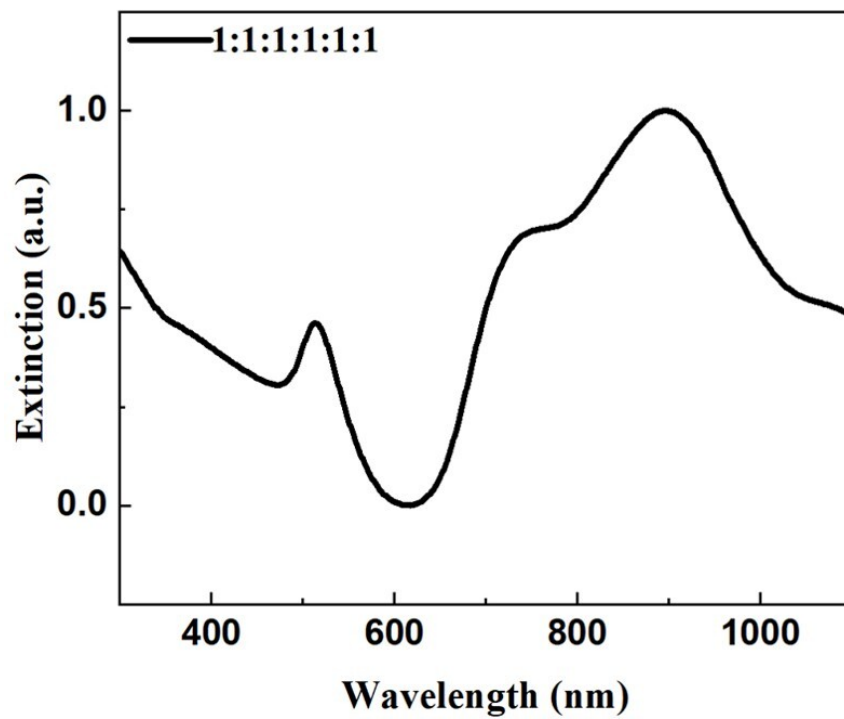


Fig. S6 The calculated spectrum of the mixed solution by the ratio of 1:1:1:1:1.

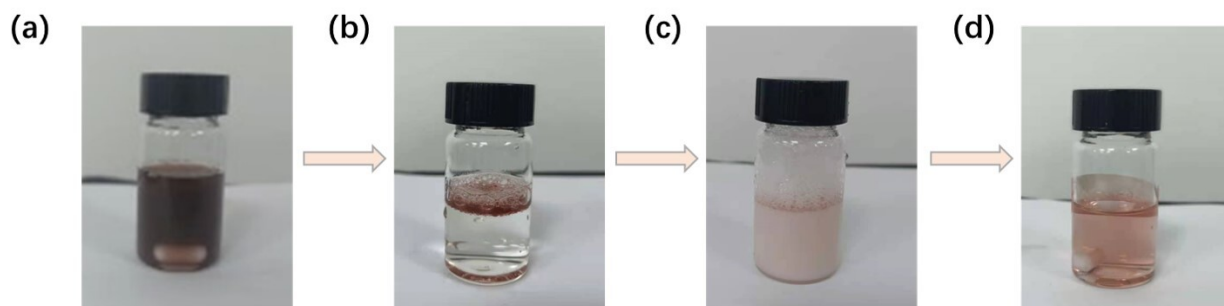


Fig. S7 Photographs of the main steps in the process of self-assembling GNRs@SiO₂ particles into superparticles. (a) The mixed GNRs@SiO₂ dispersed in ethanol solution. (b) The oil-water layered interface is made with GNRs@SiO₂@OTMS particles dispersed in cyclohexane in the upper layer and deionized water in the lower layer. (c) The emulsion obtained after sonication. (d) The broadband superparticles obtained after evaporation of cyclohexane.

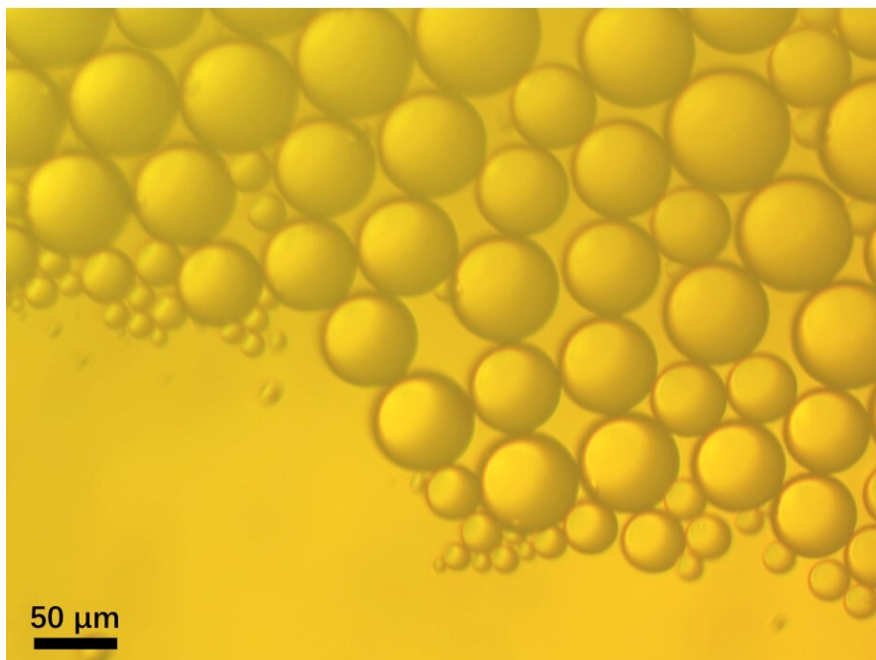


Fig. S8 The cyclohexane oil droplets in the emulsion photographed under an optical microscope with a 10x objective.

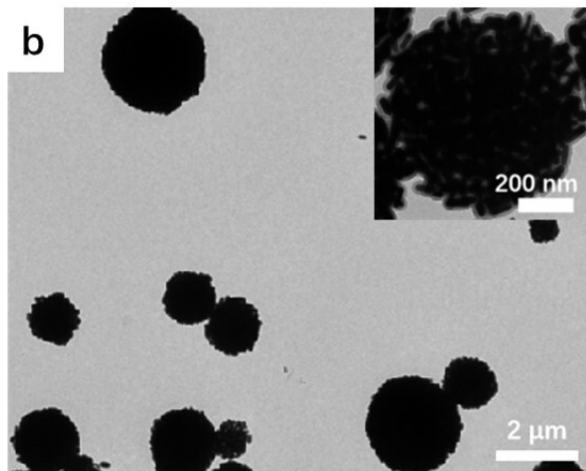
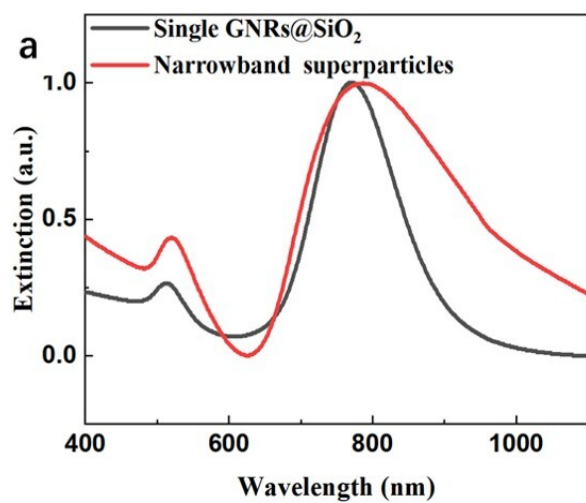


Fig. S9 Extinction spectroscopy and TEM characterization. (a) Extinction spectroscopy of single GNRs@SiO₂ (black, LSPR at 760 nm) and their corresponding superparticles (red). (b) TEM images of narrowband superparticles with average size 1.1 μm.

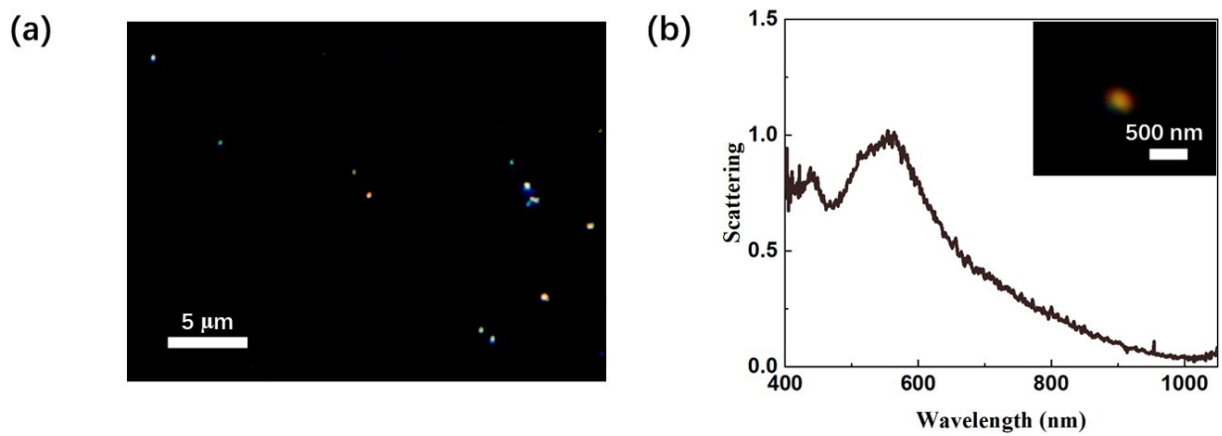


Fig. S10 GNRs@SiO₂ picture in darkfield mode and its corresponding single-particle scattering spectrum. (a) Fig. 2a1 of the GNRs@SiO₂ were prepared on a silicon wafer after dilution of 1000 times, followed by photographs taken with an Olympus BX53M optical microscope with the objective (100×, NA= 0.80). (b) The darkfield single-particle scattering spectrum of the GNRs@SiO₂, and the inset is the picture of corresponding particle taken under dark field condition.

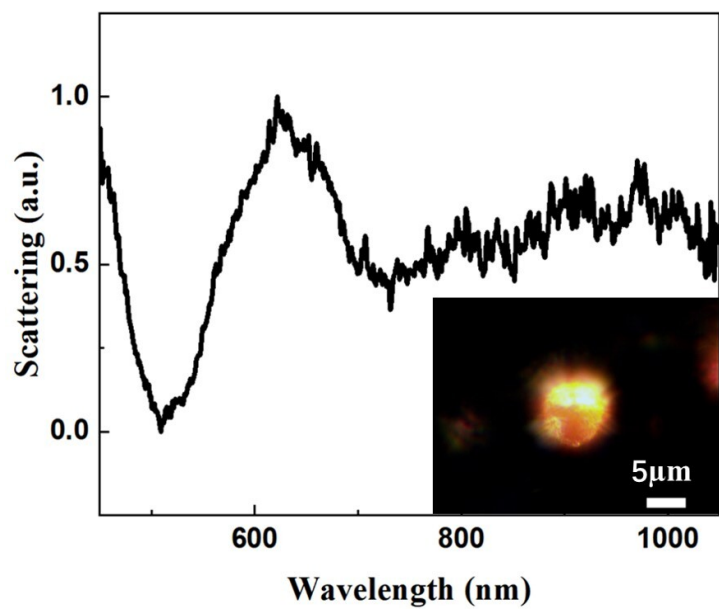


Fig. S11 Darkfield single-particle scattering spectra of broadband superparticles and corresponding photographs. The photograph was taken with an Olympus BX53M optical microscope with the objective (100 \times , NA= 0.80).

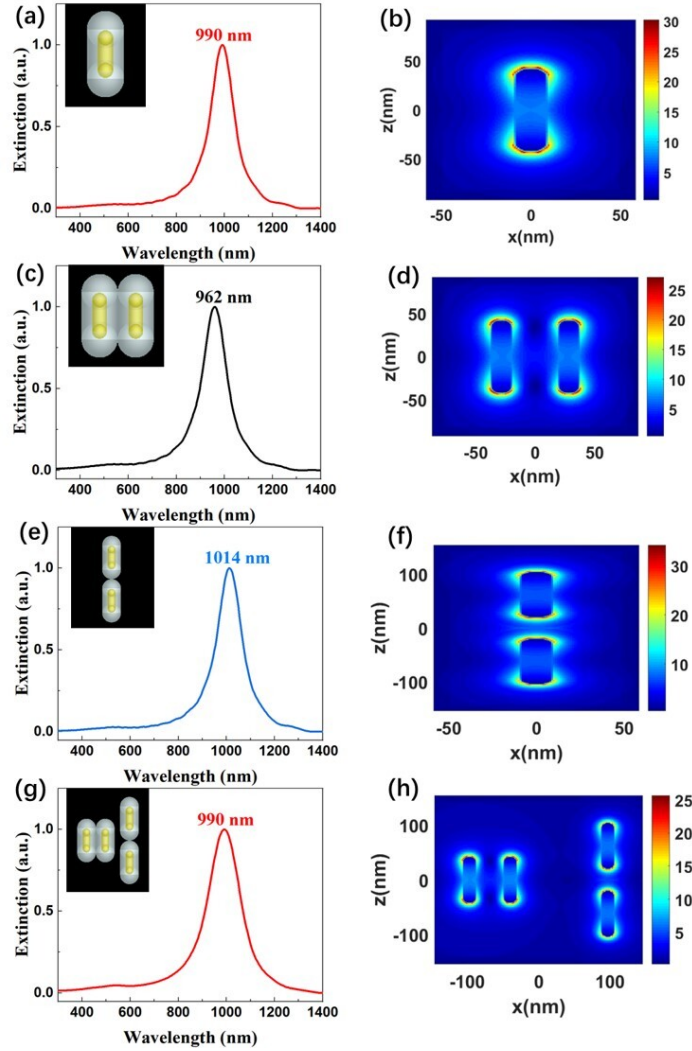


Fig. S12 The extinction spectra and electric field distributions obtained by FDTD simulations illustrate that the plasmonic coupling effect between the GNRs@SiO₂ can be ignored. (a, b) extinction spectra (a) and electric field distribution (b) of the GNRs@SiO₂ with the LSPR of 990 nm in Fig. S2b. (c, d) (c) is two GNRs@SiO₂ of the same size as the model in (a) arranged side-by-side and (d) is the corresponding electric field distribution. (e, f) (e) is two GNRs@SiO₂ of the same size as the model in (a) arranged head-to-head and (f) is the corresponding electric field distribution. (g, h) (g) is the GNRs@SiO₂ arranged side-by-side and head-to-head together, the peak position is similar to (a), and (h) is the electric field distribution.

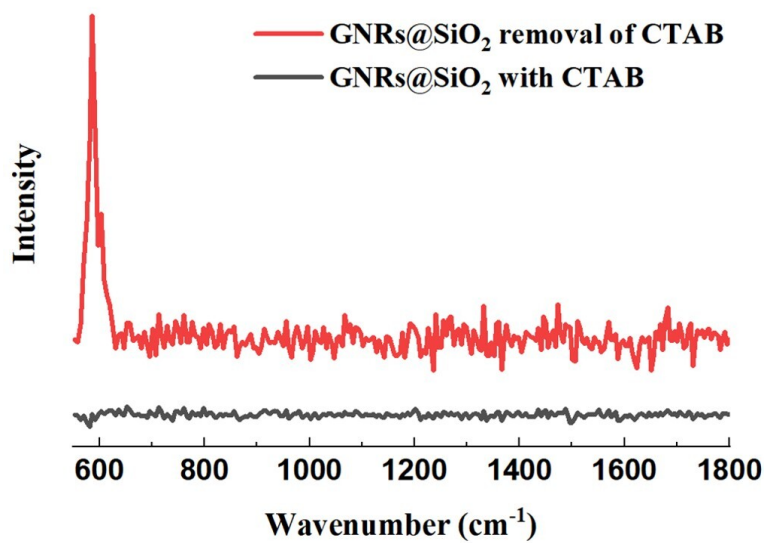


Fig. S13 Effect of removal of CTAB template on SERS performance of GNRs@SiO₂. The Raman measurements were recorded with a 785 nm laser, 200 mW laser power, 50 x air objective (NA= 0.75), 10 s exposure time and 1 accumulation per spot.

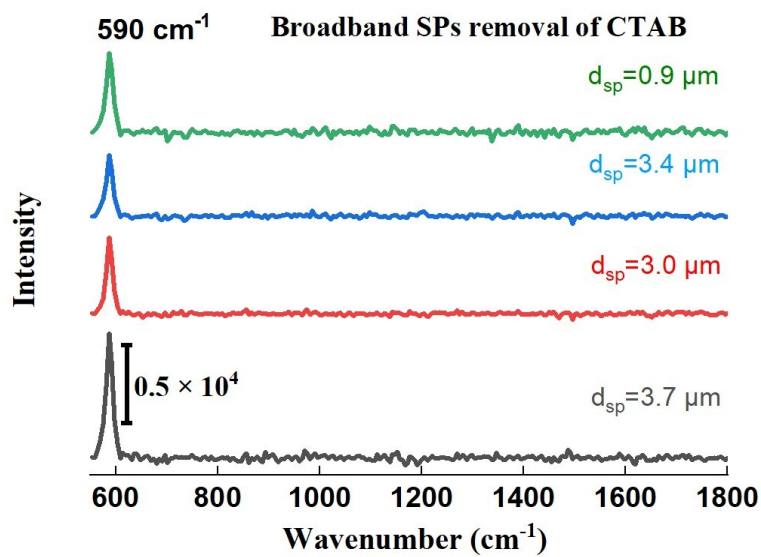


Fig. S14 SERS performance of different sizes of the GNRs@SiO₂ superparticles. The Raman measurements were recorded with a 785 nm laser, 200 mW laser power, 50 x air objective (NA= 0.75), 10 s exposure time and 1 accumulation per spot.

Table S1. Preparation parameters of 6 different sizes of GNRs and related data of measured sizes. The concentrations of AgNO₃, HAuCl₄, HCl, and AA solutions were 4 mM, 0.01 M, 12.1 M, 0.064 M.

CTAB (g)	NaOL (g)	AgNO ₃ (mL)	HAuCl ₄ (mL)	HCl (mL)	AA (mL)	Seed (mL)	Average length (nm)	Average diameter (nm)	Average AR	Fig. number
7.0	1.23	12.0	25.0	2.1	1.25	0.8	117.5±6.4	56.3±2.6	2.1±0.2	Fig. 2a1
7.0	1.23	24.0	25.0	1.5	1.25	0.4	86.8±8.3	28.2±2.0	3.1±0.4	Fig. 2a2
9.0	1.23	24.0	25.0	1.5	1.25	0.1	84.1±14.0	21.4±3.8	3.9±0.4	Fig. 2a3
9.0	1.23	24.0	25.0	2.1	1.25	0.1	90.1±5.4	20.5±1.5	4.4±0.5	Fig. 2a4
7.0	1.23	24.0	25.0	3.6	1.25	0.8	84.0±17.6	17.0±1.0	4.9±1.1	Fig. 2a5
7.0	1.23	24.0	25.0	5.4	1.25	0.8	103.0±13.3	15.7±1.8	6.6±0.9	Fig. 2a6